Trajectories of Water and Sand Jets

D.A. Serrano, F. Sánchez-Silva, J. Klapp, P. Tamayo, A. Medina and G. Domínguez

Abstract In this paper we introduce a correlation for the trajectories of sand jets, of a non-cohesive granular material, emerging from vertical sidewall orifices of diameter D and wall thickness w. A contrast with water jet in similar configurations has been performed. We found that the theoretical trajectories agree well with the experimental ones.

D.A. Serrano (✉) · F. Sánchez-Silva
ESIME Zacatenco, Instituto Politécnico Nacional, Avenida Luis Enrique Erro S/N, 07738 Zacatenco, Mexico, D.F., Mexico
e-mail: arman2390@hotmail.com

F. Sánchez-Silva
e-mail: fsanchezs@ipn.mx

P. Tamayo · A. Medina
ESIME Azcapotzalco, Instituto Politécnico Nacional, Av. de las Granjas 682, 02250 Santa Catarina, Mexico, D.F., Mexico
e-mail: ptamayom@ipn.mx

A. Medina
e-mail: amedinao@ipn.mx

J. Klapp
Departamento de Física, Instituto Nacional de Investigaciones Nucleares, La Marquesa, 52750 Ocoyoacac, Estado de México, Mexico
e-mail: jaime.klapp@inin.gob.com

J. Klapp
ABACUS-Centro de Matemáticas Aplicadas y Cómputo de Alto Rendimiento, CINVESTAV-IPN, La Marquesa, 52740 Ocoyoacac, Estado de México, Mexico

G. Domínguez
Instituto Mexicano Del Petróleo, Eje Central Norte Lazaro Cardenas No 152, Col. San Bartolo Atepehuacán, 07730 Del. Gustavo A. Madero, Mexico, D.F., Mexico
e-mail: gdzacari@imp.mx

J. Klapp et al. (eds.), *Recent Advances in Fluid Dynamics with Environmental Applications*, Environmental Science and Engineering, DOI 10.1007/978-3-319-27965-7_22

1 Introduction

Leonardo da Vinci (1452–1519), performed experimental studies of the output water force through orifices, demonstrating that the water force changes according to the location of the orifices drilled on a wall container at different heights, his results are presented in the Codex of Madrid I, (Da Vinci 1480). In addition, he showed that the water jet attains a larger distance, when the orifice is in the lowest part of the container; due to this discovery, Leonardo was capable of considering the transformation of the implicit energy in the phenomenon and had the intuition about the conservation of the total energy (Levi 1986).

It is surprisingly common to find a drawing like the one shown in Fig. 1a, included in textbooks for hydrostatic pressure explanation. This drawing represents the water jets emerging of three orifices perforated on a container wall filled with water, opened to the atmosphere. Leonardo's intention was to demonstrate that the hydrostatic pressure increases with the depth, which is a correct idea. However, the drawing experimental results shown in Fig. 1a, were widely studied and questioned by Gorazd (2011), he performed the same experiments, and observed a different result from Leonardo's prediction, actually at present this topic is still a problem under study. But in fact the predictions proposed by Leonardo are correct, for the case when the orifice is in the lowest part of the container, the water jet attains bigger distances (Planinšič 2011).

Figure 1b shows that Leonardo performed experiments, using a container filled with water, there are perforations on the lateral wall and bottom of the container, he added different nozzles to the orifices, to observe weather the exit water force is a function of the orifice position in the container lower part or the height on his walls. Leonardo observed that the force is the same; it does not depend on the position of the orifices when they are located in the bottom of the container. On the contrary, for the orifices on the container sidewall, the one located in the lower part, emerges with a bigger force, due to the higher hydrostatic pressure in this point.

In Fig. 1c, Leonardo da Vinci questioned about; "What water will come out with the greatest violence, that from nozzle a, b, or c?" The right panel depicts an experiment designed to test whether the weight of water in the container bottom varies from one point to another. The "violence" of water discharged from the different nozzles was compared with a scale suspended whose plates were stroked by the jets of water. Since the plates are represented in equilibrium, Leonardo seems to have realized that the water weight in the container bottom does not change from point to point. In the experiment shown in the central panel, Leonardo tested whether the force exerted by the water on a point at the bottom depends on the volume of the container (Cavagnero et al. 2014).

Leonardo's observations show that he has anticipated Evangelista Torricelli (1608–1647) and Daniel Bernoulli (1700–1782) by admitting that a vertical stream rises to the same level of the free surface of still water that produces it. Torricelli's theorem is a fluid dynamics theorem that relates the speed of a jet outgoing through an orifice on a container wall, under the action of gravity force (Torricelli 1641).

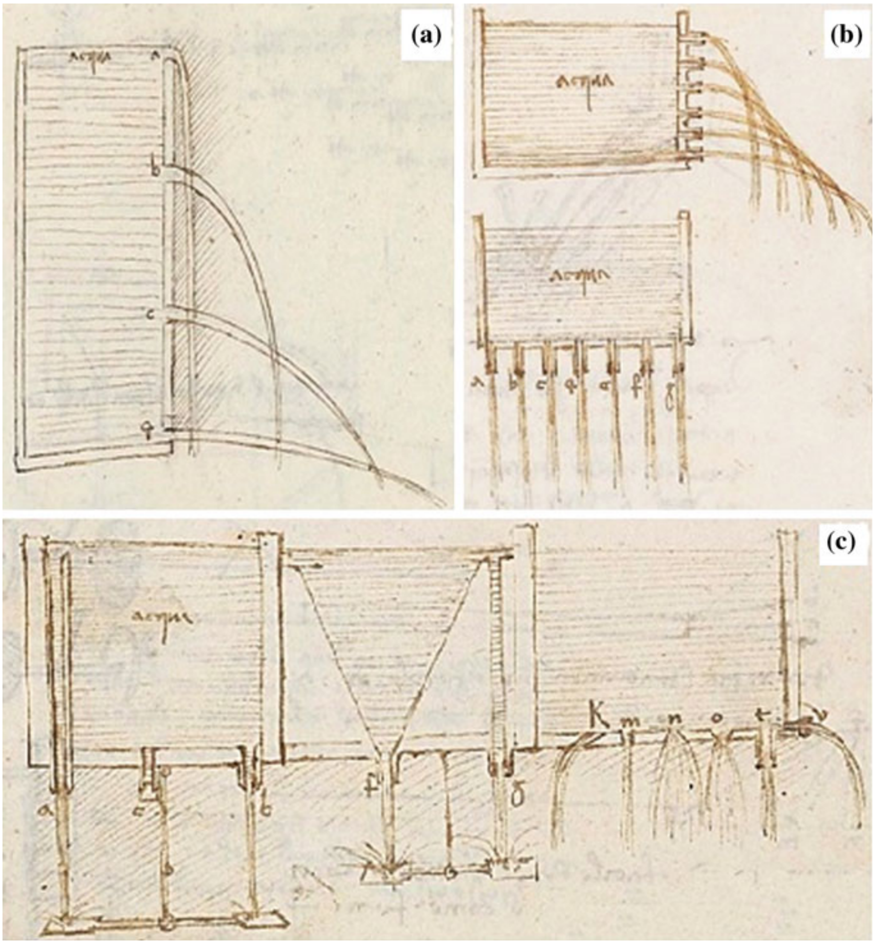

Fig. 1 Codex of Madrid I, Leonardo da Vinci performs experiments to demonstrate that: **a** the energy of the water changes according to the discharge orifice height, **b** the force of every jet in the horizontal plane is the same and **c** The weight of the water does not change from a point another

The output liquid speed through an orifice located in a container bottom is the same as the one a body acquires (in this case a drop of water) falling freely in a vacuum from a height, h, being the height of the fluid column, i.e., $v = \sqrt{2gh}$, where g is the acceleration due to gravity. Torricelli's law shows that the pressure increases when the orifice is in the lowest point of the container, producing a water jet with greater extension than the one at the top of the container.

For the experiment, at the beginning all three orifices are blocked, and then the tube is filled with water. Once the container is filled, we proceed to unlock the orifices. The jets have a static charge depending on the position they have on the wall, the exit fluid speed is higher as the orifice is located in the lower part of the

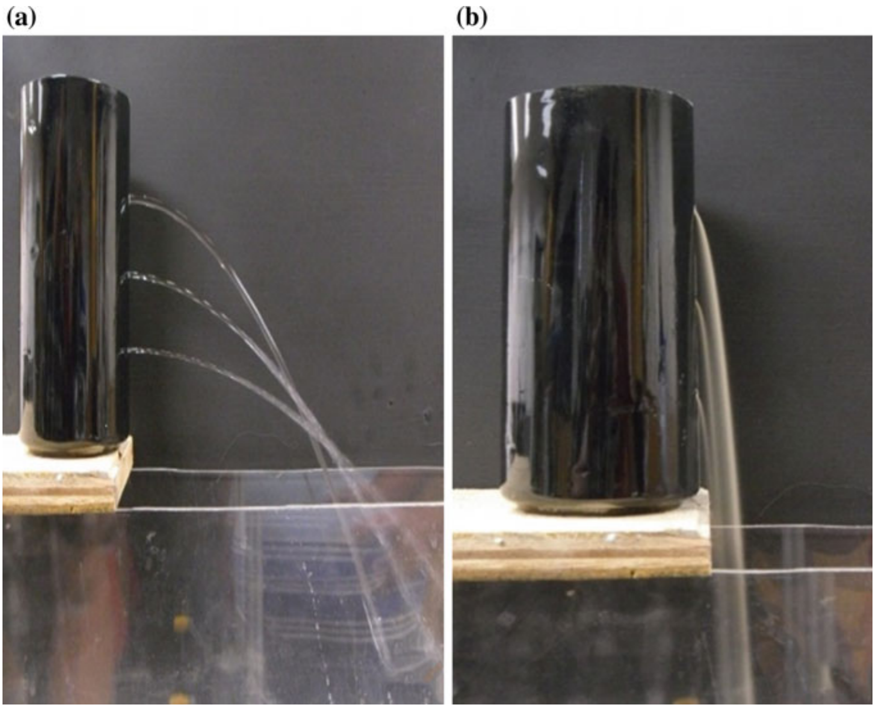

Fig. 2 Spouting can jets: liquid and non-cohesive dry sand

tube, (Fig. 2a). However, when the container is filled with dry sand and is drilled with three orifices of the same diameter, D, located as shown in Fig. 2b, the sand exit speed is the same and therefore the sand jet shape is similar in each orifice (Fig. 2b). The difference between the discharge of a container filled with dry sand and the discharge of other filled with water is that the mass flow rate, in the first case, does not depend on the orifice position, h.

The explanation most frequently used for this independence it based on the effect of the container walls geometry (Medina et al. 2013), when $\alpha > \theta_r$ the system will produce an outflow, α is the natural angle of the container wall, which can be defined as $\alpha = arctan(D/w)$ and θ_r it is the rest angle of the granular material. The sand output stream must be stopped when $\theta_r > \alpha$. Therefore a critical condition for the sand outflow is when,$\theta_r = \alpha$, the mass flow rate is proportional to $(\alpha - \theta_r)$, therefore; $\dot{m} \sim (\alpha - \theta_r)$. This is the first indication that the sand jets must be very different respect the water jets, on the other hand, the wall thickness, w, greatly affects the intensity and shape of sand jets, but this is not the case for water. In both cases, the competition between the frictional forces, the gravity force and the pressure affect the sand jet properties (Medina et al. 2013).

In this paper a discussion about the form of jets of water and sand when they outcome from the bottom of the container is presented. First, there is a brief review about the trajectories followed by water jets due to gravity when a container with sidewalls is used. Then, a theoretical development for the description of sand jets is presented and finally there is a theoretical development for the sand jet trajectories, when the container is inclined.

2 Shape of the Water Jets and Sand in Horizontal Walls

The non-cohesive dry granular materials, exhibit a behaviour that crosses the boundaries between the different states of matter. They can behave as solid, liquid or gas. In certain situations, the granular materials show features that remember the instabilities encountered in fluids, as the Faraday instability, the presence of Taylor vortices, or the Kelvin-Helmholtz instability (Melo et al. 1995; Garcimartin et al. 2002). The experimental study of instabilities of jets emerging from the bottom orifices of containers full of water or metal powder was performed by Khamontoff (1890), as shown in Fig. 3. The study of the similarities and differences between the behaviour of a liquid and a granular flow is of great importance for the understanding the subtle properties of granular flows (Boudet et al. 2007).

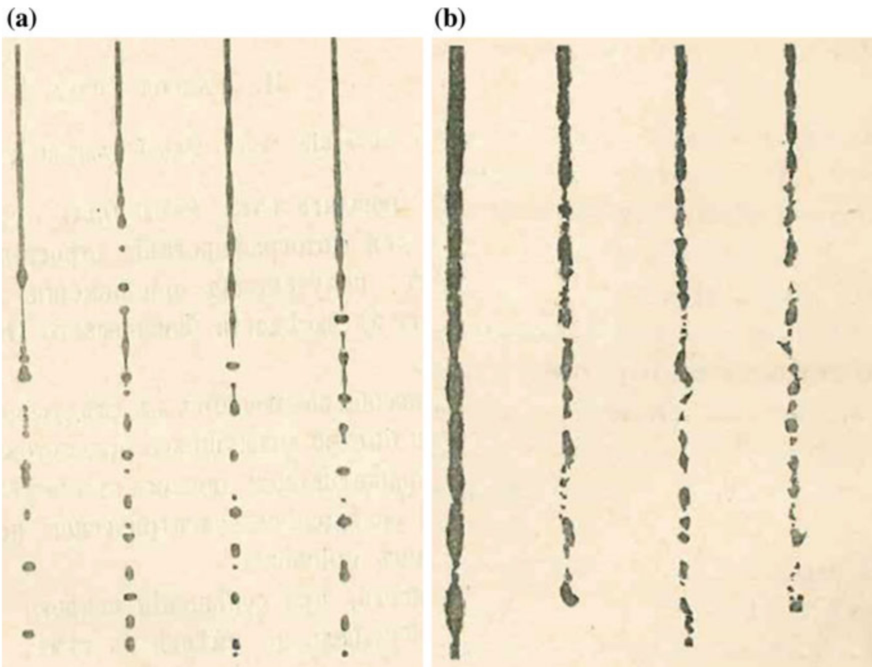

Fig. 3 From the bottom of the container: **a** water, and **b** metal powder

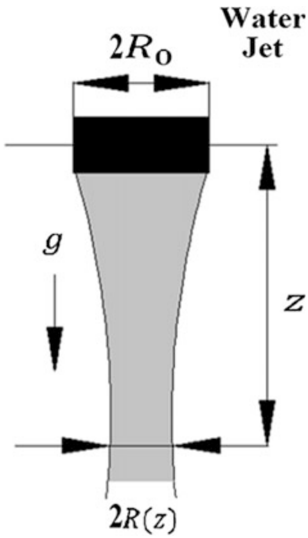

Fig. 4 Water jet emerging from the *horizontal* walls of the container

The simplest analysis about the way a water jet falls freely from the hopper by gravity, is shown in Fig. 4, it follows the application of Bernoulli's equation (the energy equation) for a water jet, in which viscosity effects and the surface tension (the pressure varying with the jet radius) are disregarded (Middleman 1995).

The continuity equation $v_i A_i = v_s A_s$, relates the speed, v, and the cross section area, A, in two different places of the water jet (subscripts "i" and "s" refer respectively to the lower and upper parts of the water jet). The water emerges from the orifice as shown in Fig. 4, it falls freely, since the nozzle exit, and its speed, $V(z)$ increases with the distance, z, being, $V^2(O)$, the output velocity of the water jet, it follows that

$$V(z) = \sqrt{2gz + V^2(O)} \tag{1}$$

The diameter $2R(z)$, shows the water jet dimensions during the water jet fall, as the jet is reduced, for different diameters of funnel, we can observe that the shape of the water jet changes as follows (Middleman 1995)

$$\frac{2R(z)}{2R_0} = \left(1 + \frac{2gz}{U_0^2}\right)^{-1/4} \tag{2}$$

Equation (2) shows how the shape of the water jet changes, once the radius R_0 and the height z, are adjusted by the diameter of the funnel. The equation is used for water jets falling from the bottom of a container (Middleman 1995).

It is possible to characterize experimentally the fall of a sand jet by using the same scheme given in Fig. 4. Due to the jet diameter reduction, the funnel formed has different radius, and the shape of the jet of granular material goes as follows (Boudet et al. 2007)

$$\frac{R(z)}{R_0} \sim \left(\frac{z}{R_0}\right)^{-1/6} \quad (3)$$

Equation (3) gives the jet shape of granular material, resulting in a universal equation once the radius $R(z)$ and the height z are adjusted by the radius of the funnel. This scaling is valid if the height z, is greater than the diameter of the funnel. The equation is used for sand jets falling from a conical hopper or orifices in horizontal walls but none theoretical model supports such a formula (Boudet et al. 2007).

3 Shape of the Water Jets from Holes on Vertical Sidewalls

Lets first study the phenomenon closely related to the trajectories of the water jets. Since the beginning, the researchers found that the distance reached by the water jet increases with the depth at which the container orifice was drilled, as shown in Fig. 5. The drawing shows a container with water at a constant level, H, water jets emerging from three orifices drilled at levels of $h = ¼\ H$, $½\ H$ *and* $¾\ H$. The intention was to demonstrate that the hydrostatic pressure influences the distance reached by the water jets (Banks 1998).

When conducting experiments about the water jet trajectories, researchers found that in the absence of air resistance, the trajectory of a basketball, for example, and the curve of a water jet are the same; both are parables. Instead, let's look at some

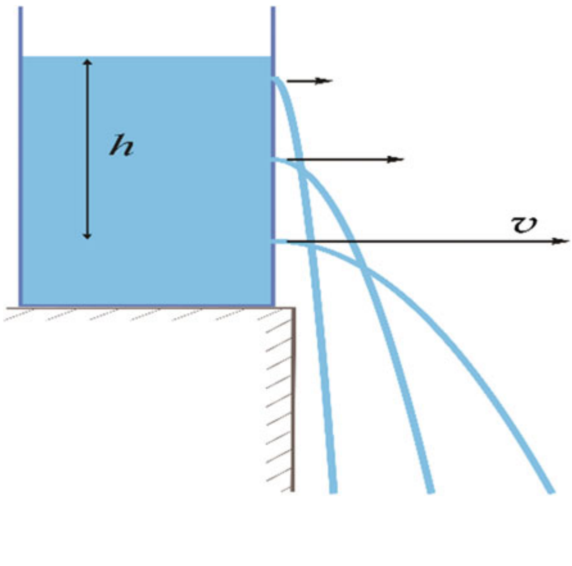

Fig. 5 Water jets from orifices on a *vertical* wall

aspects of water jets and fountains. As before, it is assumed that the effects of air resistance can be ignored, that is, the water jet is in a vacuum medium (Banks 1998). Therefore it can be analyzed using the same equation for the trajectory of a projectile Eq. (5).

$$y = (\tan\alpha)x - \left(\frac{g}{2U_0^2}\right)(\sec^2\alpha)x^2 \quad (4)$$

where U_0 is the initial velocity of the jet emerging from the hole.

In the above equation, it can be used the dimensionless parameters

$$\zeta = \frac{y}{h}$$

$$\eta = \frac{x}{h}$$

In Eq. (4), α is the exit angle, which may be positive or negative depending on the outlet orifice of the water jet (Lopac 2015), g is the gravity acceleration and $x,$ is the trajectory followed by the water jet. Using the dimensionless parameters above presented ζ and $\eta,$ and including the definition of the Froude number ($Fr = 2U_0^2/hg$), the dimensionless resulting equation is

$$\zeta = \eta(\tan\alpha) - \left(\frac{\eta^2}{Fr}\right)(\sec^2\alpha) \quad (5)$$

4 Shape of Sand Jets in Vertical Walls

As shown in Fig. 6, the container has a wall angle α, which depends on the wall thickness w. Figure 6a shows schematically a container with vertical sidewalls, on one of them there is an exit orifice of diameter, $D,$ through which the granular

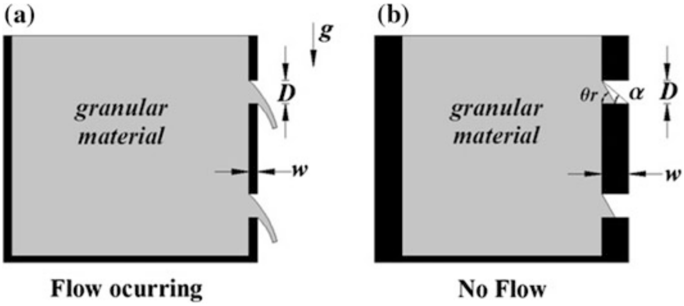

Fig. 6 Schematic side outlet of a vertical wall container in view

material flows. Figure 6b, also shows that there is a natural angle of the wall, α, which can be defined as; $\alpha = atan(D/w)$, reported in previous studies (Medina et al. 2013). The same figure also shows that there is no flow of granular material when the wall thickness is large enough, the material remains there until it reaches its angle of repose, θ_r, therefore, an outflow will occur only if $\alpha > \theta r$, as also has been noted by Woodcock and Mason (1987).

The actual study considers a dry non-cohesive granular material; sand density is much higher than the density of air, $\rho \gg \rho_a$, the output of the sand jet is a function of the angle of repose of the granular material and not of the container wall angle. Under these hypotheses, the Eqs. (6) and (7) of the momentum of Newton in both directions, are the same as in a linear approximation, so then they can be written as follows.

$$\frac{d^2x}{dt^2} = 0 \tag{6}$$

$$\frac{d^2y}{dt^2} = g \tag{7}$$

In these equations, t is the time and (x, y) are the coordinates of any point on the trajectory of the granular stream. Equations (6) and (7) represent an initial value problem, with the following conditions for an initial time $t = 0$.

$$\begin{array}{ll} x = 0; & u_x = U_0 cos\theta_r \\ y = 0; & v_y = U_0 sin\theta_r \end{array} \tag{8}$$

where U_0, is the initial velocity of the sand jet at the origin $(x = 0, y = 0)$. Using the initial conditions of the sand jet in the equations of momentum of Newton, and establishing the mass flow rate emerging from the container vertical wall $\dot{m} = c\dot{m}_0(\alpha - \theta_r)$, where the mass flow rate is equal to $\dot{m}_0 = \rho g^{1/2} D^{5/2}$ (Medina et al. 2013), the output speed of the mass flow rate is

$$U_0 = \frac{\dot{m}}{\rho A} \tag{9}$$

In the above equation A is the area of the circular orifice outlet of granular material $A = \pi D^2/4$, then the output speed is

$$U_0 = \frac{4c}{\pi} \sqrt{gD}(\alpha - \theta_r) \tag{10}$$

By using the initial conditions (8) and Eq. (10), in the momentum Eqs. (6) and (7), the trajectory for the sand jet is obtained as

$$y = \frac{\pi^2}{32c^2(\alpha - \theta_r)^2}\left(sec^2\theta_r\right)\left(\frac{x}{\sqrt{D}}\right)^2 + x\tan\theta_r \tag{11}$$

where c, is a constant of the material properties. By doing the dimensionless analysis and considering the following dimensionless variables for the sand jet trajectories equation,

$$\psi = \frac{y}{D}, \quad \chi = \frac{x}{D},$$

once the above dimensionless variables are replaced in the Eq. (11), the equation for the trajectories of the sand jet of the path of blasting is obtained

$$\psi = \frac{\pi^2}{32c^2(\alpha - \theta_r)^2}\left(sec^2\theta_r\right)\chi^2 + \chi\tan\theta_r \tag{12}$$

In previous studies about the estimation of the mass flow rate of granular material through vertical walls, (Medina et al. 2013), constructed a rectangular container with vertical walls of different thickness and outlet orifice diameter size. They observed that the output of granular material (beach sand) can be affected by the wall thickness and size of the orifice, as shown in Fig. 7.

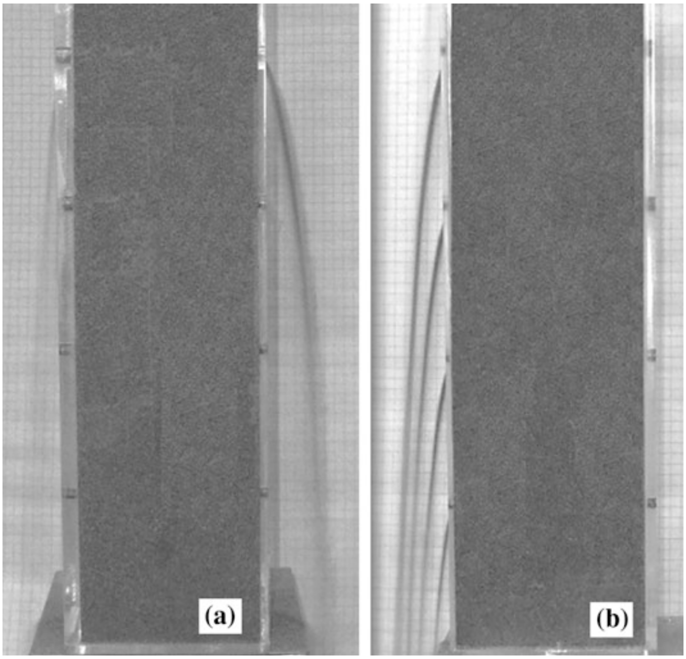

Fig. 7 Trajectory of the sand jet affected by the wall thickness and the diameter size of the orifice

By plotting Eq. (11), we can analyze the sand jets trajectories, considering the following cases:

(a) wall thickness very small (almost zero) $w = 0.01$ cm, for orifice diameters $D = 0.2, 0.25, 0.5$ and 0.6 cm.
(b) different wall thickness, $w = 0.3, 0.4, 0.6$ and 0.9 cm, the outlet orifice diameter was kept constant $D = 1$ cm.
(c) different orifice diameters, $D = 1.0, 0.8, 0.7$ and 0.5 cm the wall thickness was kept constant $w = 0.6$ cm.

In the plot of Fig. 8a, the wall thickness is very small, $w = 0.01$ cm, with the orifice diameter $D = 0.2$ cm, there is a decrement of the sand jet and a shorter extension range. If the diameter is $D = 0.6$ cm, there is an increment in sand jet and the jet is also wider, as shown in Fig. 2b, when the wall thickness is very small the shape and extension of the sand jet is a function of the exit orifice diameter.

In the plot of Fig. 8b, the orifice diameter on the wall container is constant of, $D = 1$ cm, for the wall thickness $w = 0.9$ cm, the sand jet comes out with a reduction and a shorter extension range, as shown in Fig. 7a, left sidewall of the container. For the wall thickness $w = 0.3$ cm, the sand jet comes out with greater intensity and longer extension range, as shown in Fig. 8b, left sidewall of the container, the wall thickness affects the intensity and extension of the sand jet.

The plot in Fig. 8c considers a constant wall thickness $w = 0.6$ cm, and varying the diameters of the outlet orifice. For the diameter $D = 1$ cm, the sand jet attains a longer extent than the jet for diameter $D = 0.6$ cm, as seen in Fig. 7b, left side of the sand container. The sand jet emerges with the same intensity, but when the orifice diameter is bigger the extent is larger.

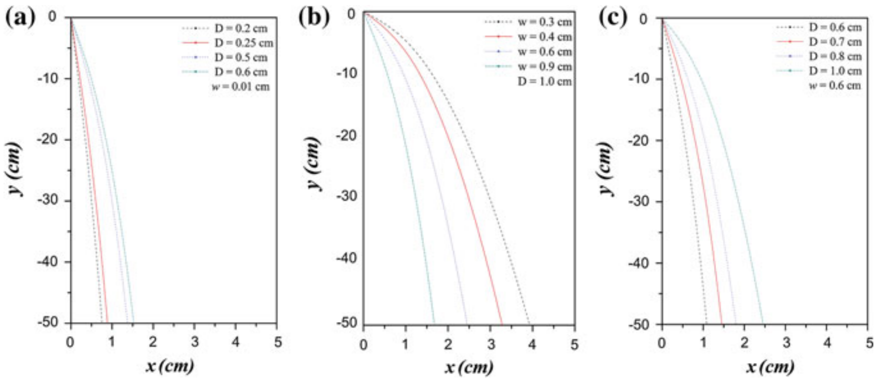

Fig. 8 Trajectory of the sand jets, **a** for different orifice diameters and a wall thickness w = 0.01 cm, **b** for different wall thickness and D = 1.0 cm and **c** for different orifice diameters and a wall thickness w = 0.6 cm

5 Conclusions

In this paper, the trajectories of water and sand jets were analysed for different situations but mainly for orifices on vertical sidewalls. The sand jet trajectories and their extension are represented well using Eq. (11). In previous work to estimate the mass flow rate of granular material through vertical walls of a silo, we note that the intensity and extension of the sand jet can be affected by the wall thickness and the orifice diameter in the jet outlet, as shown in three cases carefully discussed. To our knowledge this kind of studies, for these specific regimes, are for the first time discussed in the specialized technical literature.

Acknowledgments Authors wish to thank the IPN support through the project 20150815 (mathematical model to simulate dynamically an aero condenser used in thermoelectrical power plants) and the project 20151924 (PIV submerged jet).

References

Banks R (1998) Towing icebergs, falling dominoes and other adventures in applied mathematics. Princeton University Press, Princeton

Boudet JF, Amarouchene Y, Bonnier B, Kellay H (2007) The granular jump. J Fluid Mech 572:413–431

Cavagnero P, Revelli R (2014) The weight of water. Phys Today 67:41–46

Da Vinci L (1480) Codex Madrid I, Biblioteca Nacional de España. http://leonardo.bne.es/index.html

Garcimartin, A, Maza D, Ilquimiche JL, Zuriguel I (2002) Convective motion in a vibrated granular layer. Phys Rev E 65:031303-1–031303-5

Khamontoff N (1890) Application of photography to the study of the structure of trickles of fluid and dry materials. J Russ Physico-Chem Soc Saint Petersburg 22:281–284

Levi E (1986) El agua según la ciencia Evolución de la hidráulica. Series del Instituto de Ingeniería UNAM, Mexico

Lopac V (2015) Water jets from bottles, buckets, barrels, and vases with holes. Phys Teacher 53:169–173

Medina A, Serrano DA, Gutiérrez GJ (2013) On the mass flow rate from silos with lateral exit holes. Rev Mex Fis 59:287–291

Melo F, Umbanhowar P, Swinney HL (1995) Hexagons, kinks, and disorder in oscillated granular layers. Phys Rev Lett 75:3838–3841

Middleman S (1995) Modeling axisymmetric flows, dynamics of films, jets, and drops. Academic Press, San Diego

Planinšič G, Ucke C, Viennot L (2011) MUSE group (More Understanding with Simple Experiments) in the Physics Education Division (PED) of the European Physical Society (EPS). http://education.epsdivisions.org/muse/

Torricelli E (1641) Opera Geometrica. https://archive.org/details/operageometrica44900torrgoog

Woodcooks CR, Mason JS (1987) Bulk solids handling, an introduction to the practice and technology. Chapman and Hall, New York